Tetrahedron 69 (2013) 4922–4932

Contents lists available at SciVerse ScienceDirect

Tetrahedron

journal homepage: www.elsevier.com/locate/tet

Facile syntheses of disubstituted bis(vinylquinolinium)benzene derivatives as G-quadruplex DNA binders

Zhen-Quan Liu, Shi-Tian Zhuo, Jia-Heng Tan, Tian-Miao Ou, Ding Li, Lian-Quan Gu, Zhi-Shu Huang *

School of Pharmaceutical Sciences, Sun Yat-sen University, Guangzhou 510006, People's Republic of China

ARTICLE INFO

Article history:
Received 12 January 2013
Received in revised form 28 March 2013
Accepted 11 April 2013
Available online 16 April 2013

Keywords:
Bisquinolinium derivatives
One-pot reaction
S_NAr reaction
G-quadruplex
Binding agents

ABSTRACT

A series of disubstituted bis(vinylquinolinium)benzene derivatives were designed, which were prepared through a facile three-component one-pot reaction in good yield. FRET results showed that 1,3-disubstituted benzene derivatives had much stronger stabilization effect on G-quadruplex DNA than that of 1,4-disubstituted benzene derivatives. The introduction of substituted amine side chain at quinolinium obviously increased the binding affinity of compounds to G-quadruplex DNA. It was also found that 1,3-disubstituted benzene derivatives and 1,4-disubstituted benzene derivatives had different effects on the conformation of G-quadruplex DNA by CD spectroscopy analysis. The differences for the interactions of these two classes of compounds with G-quadruplex were further studied and elaborated through molecular modeling experiments.

1. Introduction

Guanine-rich sequences can self-associate into planar guanine quartets (G-quartets) that stack on each other to form unusual structures called G-quadruplexes.[1] Studies revealed the prevalence of G-quadruplex-forming sequences in promoter regions,[2] such as *c-myc*,[3] *c-kit*,[2d,4] and *k-ras*,[5] as well as in the telomeric chromosomal terminals.[6] The formation or stabilization of G-quadruplexes in these regions may play important role in the regulation of gene expression and the maintenance of telomere length. For example, formation of quadruplex structures at the promoter regions can regulate gene expression at the transcriptional level.[7] Formation of a quadruplex at the telomeric end can stop the function of the telomerase enzyme.[8] Small molecules that can selectively induce G-quadruplex formation or stabilization are therefore promising lead compounds for cancer treatment.[7,9]

Up to now, several classes of G-quadruplex ligands have been developed. Most of them share a common planar aromatic core, interacting with the terminal G-tetrad via π–π stacking. One notable class of potent G-quadruplex ligands is bisquinolinium derivatives, such as **360A** (Fig. 1) with a amide linkage between quinolinium moiety and pyridine ring, and the positive charge on quinolinium might be interacted with phosphate groups of the DNA backbone.[10] Czerwinska et al. have reported that 1,4-bis-(vinylquinolinium) benzene (Fig. 1) with a vinyl linkage between quinolinium moiety and benzene ring as a G-quadruplex binder, can be controlled to recognize parallel and anti-parallel G-quadruplex DNA by switching light.[11] In the year of 2010, our group has also reported a series of bisaryldiketene derivatives **M1**–**M4** with a vinyl linkage (Fig. 1) as effective *c-myc* G-quadruplex DNA binders with high selectivity for G-quadruplex over duplex DNA.[12] In addition, Müller et al. have reported a series of pyridostatin analogues as telomeric G-quadruplex DNA ligands and demonstrated that introduction of amine side chain would increase the stabilizing ability and selectivity of compounds to G-quadruplex.[13]

Based on the ligands mentioned above, we known that the introduction of amine side chain would increase the affinities of ligands for G-quadruplex DNA and improve their selectivity for G-quadruplex because the amine side chain may dock onto the groove of G-quadruplex DNA and interact with the G-quadruplex DNA by forming intermolecular hydrogen bond or electrostatic interaction. On the other hand, the quinolium scaffold would also interact with G-quartet plane by π–π stacking or with the phosphate backbone via electrostatic interaction. Considering that those bisquinolinium derivatives mentioned above were all bisquinolinium derivatives with a central aromatic core and the bisaryldiketene derivatives reported by our group were ones with a central alicyclic ketone. So

Abbreviations: CD, circular dichroism; FRET, fluorescence resonance energy transfer; PPA, polyphosphoric acid; S_NAr, nucleophilic aromatic substitution reaction.

* Corresponding author. Tel./fax: +86 20 39943056; e-mail address: ceshzs@mail.sysu.edu.cn (Z.-S. Huang).

0040-4020/$ – see front matter © 2013 Elsevier Ltd. All rights reserved.
http://dx.doi.org/10.1016/j.tet.2013.04.045

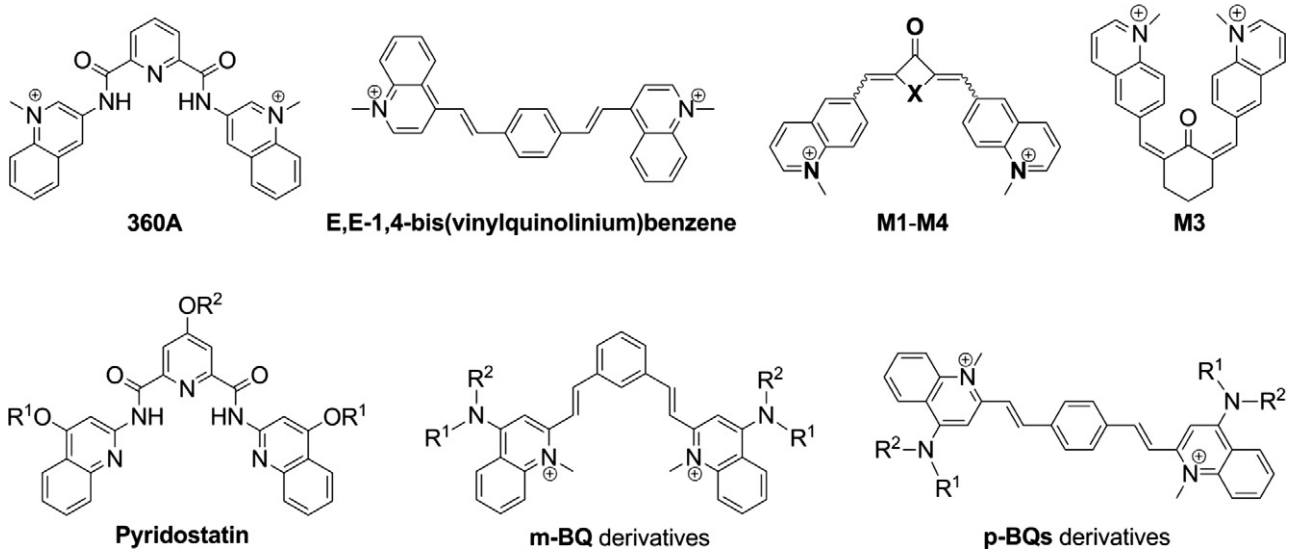

Fig. 1. Structures of the previously reported bisquinolinium G-quadruplex ligands (**360A**, *E*,*E*-1,4-bis-(vinylquinolinium)benzene, **M1**−**M4**, and *pyridostatin* derivatives) and designed target compounds (**m-BQ** and **p-BQ** derivatives).

we plan to modify the bisaryldiketene derivatives **M1**−**M4** by changing the central part with an aromatic benzene core. To the best of our knowledge, bisquinolinium derivatives with amine side chain at C-4 position of the quinolinium ring have not been synthesized and characterized as G-quadruplex binders so far. Herein, we designed a series of disubstituted bis(vinylquinolinium)benzene derivatives, which were prepared through a facile three-component one-pot reaction. As shown in Scheme 1, we successfully prepared the target compounds by combining a nucleophilic aromatic substitution reaction (S_NAr reaction) with a Knoevenagel reaction together in one-pot. By using this method, we introduced two quinolinium cores and two amine side chains to the target molecules through one-step reaction. In order to explore the effect of molecular shape on stabilization and conformation of G-quadruplex DNA, we prepared not only a series of 1,3-disubstituted benzene bisquinolinium derivatives (**m-BQ** derivatives) but also a series of 1,4-disubstituted benzene bisquinolinium derivatives (**p-BQ** derivatives). And their interactions with G-quadruplex DNA were investigated by using FRET-melting, FID assay, CD spectroscopy, and molecular modeling study.

2. Results and discussion

2.1. Chemistry

As shown in Scheme 1, in order to prepare **m-BQ** and **p-BQ** derivatives, we must firstly obtain the intermediate **3**. 2-Methyl-4-hydroxylquinoline (**1**) was prepared by condensation reaction of starting material aniline with ethyl acetoacetate catalyzed by polyphosphoric acid (PPA) at 130 °C in 77% yield. Then compound **1** was treated with phosphorylchloride at 120 °C for 2 h to give 4-chloro-2-methylquinoline (**2**) in 65% yield. Finally, 4-chloro-2-methylquinoline was methylated using methyl iodide to give a mixture of 1,2-dimethyl-4-chloroquinolinium iodide (**3**) and 1,2-dimethyl-4-iodoquinolinium chloride (**4**) with a total yield of 90%. It was found that the ratio of two compounds was 2:1 according to ^{1}H NMR and MS analysis. Considering that this mixture has no effect on next step reaction, the mixture was used directly without further purification.

For the synthesis of target compounds, a model reaction was chosen to optimize reaction condition using 1,3-benzenedicarboxyaldehyde, intermediates **3** and **4**, and pyrrolidine as starting

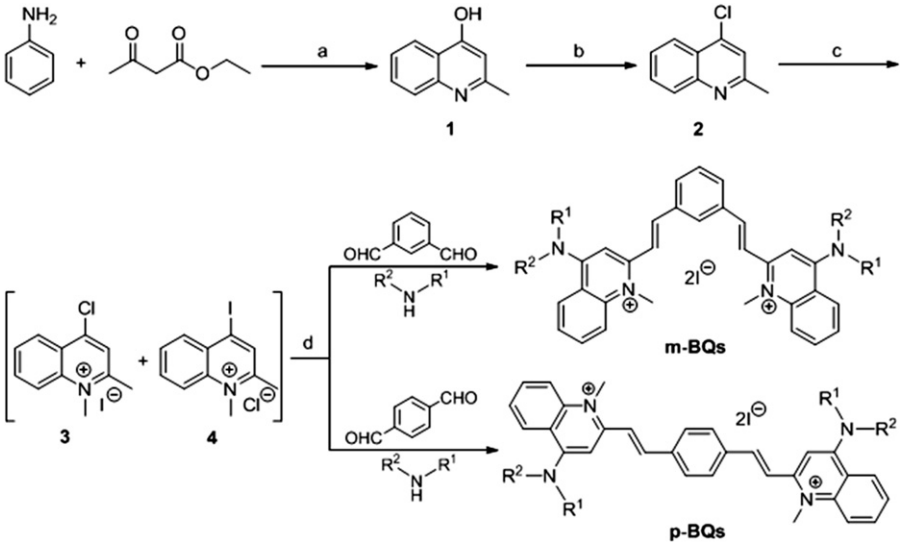

Scheme 1. Synthetic routes for bisquinolinium derivatives (**m-BQ** and **p-BQ** derivatives): (a) PPA, 130 °C; (b) $POCl_3$, 120 °C; (c) CH_3I, sulfolane, 80 °C; (d) solvents, reflux.

materials. According to the method reported by Mullins et al.[14] and considering the reactivity of our substrate, we carried out the reaction at 80 °C. The solvent for the reaction was tested with xylene, dioxane, THF, *n*-butanol, and ethanol. Our experimental results demonstrated that compounds **3** and **4** were converted to an S_NAr product in the solvents of xylene, dioxane, and THF. Especially in solvent THF, compounds **3** and **4** were reacted with pyrrolidine and converted almost completely to an S_NAr product. In ethanol and *n*-butanol, the target compound could be obtained by combining an S_NAr reaction and a Knoevenagel reaction together in one-pot with a good yield of 92% in ethanol and 50% in *n*-butanol, respectively. These results indicated that protic solvent favored the three-component one-pot reaction, and aprotic solvent only favored the S_NAr reaction. This is consistent with the results reported by Yamashita et al.,[15] which have shown that alcohol can accelerate Knoevenagel reaction. Our results indicated that the polarity of solvent had a significant effect on the reaction, and ethanol was found to be the best solvent for this reaction.

By using the above reaction, a series of **m-BQ** derivatives were prepared with starting materials 1,3-benzenedicarboxyaldehyde, 1,2-dimethyl-4-chloroquinolinium iodide, and various amines (as shown in Table 1) including cyclic aliphatic and acyclic aliphatic amines. As shown in Table 1, entries 1 to 4, cyclic aliphatic amines were generated with good yield ranging from 74 to 92%. Our results also showed that acyclic aliphatic amines were generated with a relatively low yield. As shown in entries 5 and 6 of Table 1, when N^1,N^1-dimethylethanediamine and N^1,N^1-diethylethanediamine were used as reagents, reactions led to yields of 55 and 52%, respectively, at a higher temperature of 120 °C. When cyclic amines were used, a lower temperature of 80 °C could be used. It was shown that reactive activity of cyclic aliphatic amines was much stronger than that of acyclic amines, which is consistent with the nucleophilicity of these amines.

In order to explore the effect of molecular shape on the interaction of compound with G-quadruplex, a series of **p-BQ** derivatives were also prepared by using 1,4-benzenedicarboxyaldehyde to replace 1,3-benzenedicarboxyaldehyde. As shown in Table 1, the result was similar to that of the V-shaped bisquinolinium derivatives, which gave a higher yield (from 68 to 92%, entries 1–4) for the cyclic aliphatic amines and a lower yield for acyclic aliphatic amines (51% yield in entry 5 and 62% yield in entry 6).

In addition, two bisquinolinium derivatives, **m-BQ-4O** and **p-BQ-4O**, without amine side chain were synthesized, which were used as the referenced compounds for the test. According to the coupling constant of 16 Hz for the double bond protons, the configuration of exocyclic double bond of the derivatives was identified as *E*-form.

2.2. Stabilizing ability and selectivity studies with FRET

The stabilizing ability of these bisquinolinium derivatives on G-quadruplex DNA was evaluated with FRET-melting experiments.[16] F21T (human telomeric G-quadruplex DNA), F22T (*c-myc* promoter G-quadruplex DNA), F-c-kit1-T (*c-kit*1 promoter G-quadruplex DNA), and F10T (hairpin duplex DNA) containing fluorophores at both 5′-end and 3′-end, were used in this assay. The

Table 1
Synthesis of V-shaped (**m-BQs**) and linear-shaped (**p-BQs**) disubstituted bisquinolinium derivatives

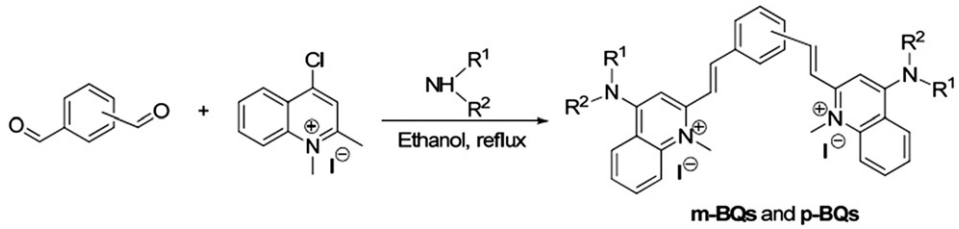

m-BQs and **p-BQs**

Entry	HNR^1R^2	Conditions[a]	Product	Yield[b] (%)
1		80 °C, 3 h	**m-BQ-Pyrro** **p-BQ-Pyrro**	92 92
2	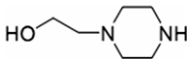	80 °C, 3 h	**m-BQ-OHEtP** **p-BQ-OHEtP**	78 68
3		80 °C, 3 h	**m-BQ-Mor** **p-BQ-Mor**	91 91
4	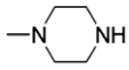	80 °C, 3 h	**m-BQ-MP** **p-BQ-MP**	74 75
5[c]	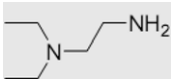	120 °C, overnight	**m-BQ-DE-EA** **p-BQ-DE-EA**	52 51
6[c]	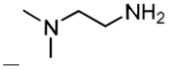	120 °C, overnight	**m-BQ-DM-EA** **p-BQ-DM-EA**	55 62
7[d]	—	80 °C, 3 h	**m-BQ-4O** **p-BQ-4O**	95 93

[a] Isophthalaldehyde or terephthalaldehyde (1.0 mmol, 1.0 equiv), 1,2-dimethyl-4-chloroquinolinium iodide (2.0 mmol,2.0 equiv), amines (2.5 equiv) and the reaction was performed at the specified temperature and for the specified length of time. All data are averaged by two experiments.
[b] Yields were obtained by measuring the product after filtering off the reaction mixture and washing with ethanol.
[c] Both reaction entries 6 and 7 were carried out at 120 °C in a sealed tube.
[d] **m-BQ-4O** and **p-BQ-4O** were synthesized by using isophthalaldehyde or terephthalaldehyde (1.0 mmol, 1.0 equiv), 1,2-dimethylquinolinium iodide (2.0 mmol, 2.0 equiv), piperidine (0.5 equiv) as starting material.

melting temperatures of all G-quadruplexes were determined in the presence of 1.0 μM of bisquinolinium derivatives in Tris–HCl buffer containing 60 mM KCl. The enhanced melting temperatures (ΔT_m) were obtained as shown in Table 2.

Table 2
Change in DNA melting temperatures (ΔT_m) determined by FRET-melting experiment[a]

Ligands	F21T[b] (ΔT_m/°C)	F22T[b] (ΔT_m/°C)	F-c-kit1-T[b] (ΔT_m/°C)	F10T[b] (ΔT_m/°C)
M3[c]	10[c]	9[c]	17[c]	0[c]
m-BQ-4O	6.1±0.7	6.0±0.4	6.2±0.5	0.0±0.2
m-BQ-Mor	19.0±0.8	10.9±0.4	16.3±0.1	0.5±0.1
m-BQ-Mp	20.3±0.1	12.5±0.3	19.3±0.2	0.7±0.3
m-BQ-OHEtP	16.8±1.0	≥16.3±0.1	20.2±1.0	0.8±0.4
m-BQ-Pyrro	8.42±0.2	14.0±0.1	7.7±1.0	0.3±0.3
m-BQ-DE-EA	9.0±0.1	7.9±0.2	−8.7±0.8	0.6±0.1
m-BQ-DM-EA	9.0±0.3	7.9±0.4	−5.5±0.5	0.8±0.4
p-BQ-4O	2.4±0.4	2.4±0.5	3.3±0.1	0.5±0.1
p-BQ-Mor	4.8±0.2	4.5±0.9	3.3±0.1	0.5±0.1
p-BQ-Mp	2.8±0.3	5.3±0.1	4.8±0.1	0.5±0.1
p-BQ-OHEtP	9.3±0.1	10.0±0.8	4.7±0.9	1.4±0.1
p-BQ-Pyrro	3.5±0.3	8.6±0.2	7.5±0.6	−0.3±0.3
p-BQ-DE-EA	1.8±0.6	4.9±0.3	2.8±0.3	0.5±0.1
p-BQ-DM-EA	2.5±0.2	4.8±0.4	3.1±0.1	0.6±0.2

[a] $\Delta T_m = T_m$(DNA+ligand) − T_m(DNA). In the absence of ligand, T_m values of annealed F22T, F21T, F-c-kit1-T, and F10T are 78.0, 60.8, 56.7, and 61.9 °C, respectively.
[b] The primary structures of all oligomers used in this study were shown in Supplementary data.
[c] Reported in Ref. 12.

The FRET-melting data (Table 2 and Fig. S1) showed that the ΔT_m values for all compounds were in a wide range from 0.6 to 20.3 °C. Most of the compounds were stabilizer of G-quadruplex DNA. The FRET results indicated that **m-BQ** derivatives had obviously higher stabilizing ability to G-quadruplex than the corresponding **p-BQ** derivatives, which suggested that the molecular shape made an important contribution for the compounds to interact with G-quadruplex. The data also showed different class of amines has varying effect in stabilizing G-quadruplex. The compounds with rigid cyclic amine displayed stronger stabilization ability for G-quadruplex than those with flexible acylic amine.

Comparing with the reference compound **M3** (a 1,3 'V'- shaped bisquinolinium derivative) that we reported previously,[12] **m-BQ** derivatives **m-BQ-Mor**, **m-BQ-Mp**, and **m-BQ-OHEtP** showed stronger stabilization ability to G-quadruplex DNA than that of **M3**, and the **p-BQ** derivatives showed weaker stabilization ability than that of **M3**.

Moreover, these derivatives had weak effect on the thermal stability of the duplex DNA F10T (Table 2 and Fig. S1, $-0.3\pm0.3\ °C \le \Delta T_m \le 1.4\pm0.1\ °C$), which implied that the derivatives had good selectivity on G-quadruplex DNA over duplex DNA.[17] Interestingly, we also found that **m-BQ-DE-EA** and **m-BQ-DM-EA** could destabilize *c-kit*1 G-quadruplex DNA structures with ΔT_m values of −8.7±0.8 °C and −5.5±0.5 °C, respectively.

2.3. Binding ability studies with FID

The binding affinities of ligands for the quadruplex and duplex structures were evaluated by using fluorescence intercalator displacement (FID) assays.[18] The assays were performed in the presence of K^+ ions with the human telomeric sequences (HTG21), *c-myc* promoter sequence Pu27, and duplex DNA ds26.

FID assay is based on the decrease in fluorescence that follows when a ligand displaces the DNA intercalator thiazole orange (TO) from a DNA structure.[19] FID curves (Fig. S2) were obtained by plotting the percentage displacement of TO against ligand concentration. The concentrations required to decrease the fluorescence by 50%, reflecting binding to quadruplex ($^{G4}DC_{50}$) or duplex ($^{ds}DC_{50}$) structures, were reported in Table 3. As the results shown in Table 3, most of synthesized **BQ** derivatives had a good G-quadruplex DNA binding ability and a relatively weak duplex DNA binding ability. **p-BQ** derivatives appear to be stronger binders for DNA than that of **m-BQ** derivatives. And comparing with the reference compound **M3**, our **BQ** derivatives showed better *c-myc* promoter G-quadruplex DNA binding ability than **M3**, which might be related to that introduction of the amine side chain into the quinolinium ring led to binding mode of ligands with G-quadruplex DNA change to a certain extent.

Table 3
Binding affinities of ligands to quadruplexes and duplex DNA measured from FID assay

Ligands	$^{G4}DC_{50}$[a] [μM]		$^{ds}DC_{50}$[a] [μM]
	HTG21	Pu27	ds26
M3[b]	0.87	1.73	12.80
m-BQ-4O	6.03	6.34	>25.00
m-BQ-Mor	6.63	1.45	41.43
m-BQ-Mp	1.32	1.18	6.00
m-BQ-OHEtP	2.15	0.83	10.89
m-BQ-Pyrro	6.16	2.09	10.29
m-BQ-DE-EA	1.76	1.56	18.8
m-BQ-DM-EA	2.12	1.55	4.39
p-BQ-4O	5.93	6.04	>25.00
p-BQ-Mor	5.3	0.83	>25.00
p-BQ-Mp	0.75	0.22	6.67
p-BQ-OHEtP	0.64	0.23	1.33
p-BQ-Pyrro	0.78	0.22	5.41
p-BQ-DE-EA	2.49	0.84	5.01
p-BQ-DM-EA	2.64	0.68	4.38

[a] DC_{50} is the ligand concentration required to displace 50% of thiazole orange (TO). Experiments were performed at least in duplicate, and estimated error values are within ±5%.
[b] Reported in Ref. 12.

2.4. Binding property studies with CD

2.4.1. Activity of compounds for inducing the formation of G-quadruplex in the presence of potassium ion. In order to investigate the activity of synthesized compounds for inducing the formation of G-quadruplex structures, the G-rich DNAs and compounds were co-annealed in the presence of 150 mM KCl, and CD experiments were carried out. CD spectroscopy is a conventional method for determining the conformation of G-quadruplex structures and the effect of ligand binding on quadruplex structure.[20] As shown in Fig. 2A and B, in the presence of 150 mM K^+, the CD spectrum of HTG21 (human telomeric G-quadruplex DNA oligomer, GGGTTAGGGTTAGGGTTAGGG) in the absence of any ligand showed a major positive band at 290 nm, a shoulder at around 270 nm, a small positive band at 250 nm, and a minor negative band near 234 nm, indicating that the formation of a mixture of anti-parallel and parallel G-quadruplexes, possibly including hybrid-types as well, which is consistent to those reported previously.[17,21] Upon the addition of different compounds to the above solution, the CD spectra changed greatly. As shown in Fig. 2A and B, most of the compounds induced the G-quadruplex DNA to mainly form a parallel structure from forms of parallel/antiparallel mixture and hybrid-type, with a positive band at 295 nm disappearance, a positive band appearance at 260 nm, and a negative band at 245 nm emergence. Only three compounds (**m-BO-4O**, **p-BQ-4O**, and **p-BQ-Mor**) induced HTG21 G-quadruplex DNA to form a similar conformation as those without these compounds. These results suggested that most of the compounds favored to induce and stabilize the HTG21 G-quadruplex DNA in form of parallel

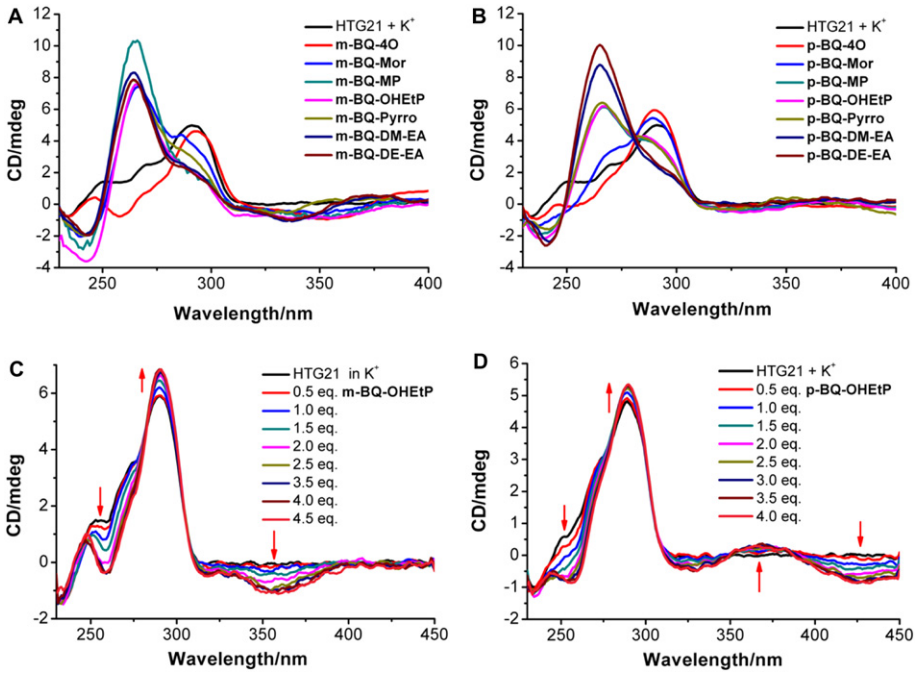

Fig. 2. CD spectra of HTG21 under the condition of 10 mM Tris–HCl (7.4) in 150 mM KCl. (A, B) Effect of the **m-BQ** or **p-BQ** derivatives on HTG21 DNA in the presence of 150 mM KCl. (C, D) CD titration spectra of compounds m-BQ-OHEtP and p-BQ-OHEtP on HTG21 DNA in the presence of 60 mM KCl.

conformation when DNA and compounds were co-annealed in the presence of 150 mM KCl.

The same experiments were carried out for oncogene promoter G-quadruplex DNA oligomer, *c-kit*1 (AGGGAGGGCGCTGGGAGGAGGG) and *c-myc* (Pu27, TGGGGAGGGTGGGGAGGGTGGGGAAGG), under the same condition mentioned above. The results shown in Fig. S3 demonstrated that most of compounds could induce and stabilize *c-kit*1 and Pu27 G-quadruplex DNAs in form of parallel structures. It was also found that on addition of **m-BQ-DE-EA** or **m-BQ-DM-EA** to the solution of *c-kit*1 G-quadruplex DNA, the CD signal intensity obviously decreased at 260 nm (Fig. S3A). As it was reported, the decrease in the CD signal suggested ligand-induced disruption of the stacking between the bases of the G-quadruplex tetrads consistent with an apparent unfolding effect. This may be due to the ability of the two compounds to recognize multiple binding sites with the G-quadruplex.[22] On the other hand, the structural differences of *c-kit*1 G-quadruplex DNA with telomeric and *c-myc* G-quadruplex DNA might be one of the most important factors to produce the results (Table S2).[23] In addition, it was also speculated that relatively flexible amino terminal in the side chain of two compounds could be more easily interact with the grooves or loops of G-quadruplex DNA, which was not conducive to the stability of G-quadruplex structure.

2.4.2. Effect of compounds on the conformation of G-quadruplex in the presence of monovalent ion. In order to further explore whether these synthetic compounds can change the conformation of G-quadruplex structures, the G-quadruplex DNA was formed by annealing in the presence of 60 mM KCl or NaCl, CD titration experiments were carried out in the presence of monovalent ions. According to FRET results, compounds **m-BQ-OHEtP** and **p-BQ-OHEtP** were selected for the following studies.

Firstly, CD titration experiments were carried out for HTG21 G-quadruplex DNA in the presence of 60 mM KCl. As shown in Fig. 2C and D, upon addition of **m-BQ-OHEtP** or **p-BQ-OHEtP** to the solution, the spectra for both didn't have obvious overall changes. A major anti-parallel structure (the positive band at 290 nm and the negative band at 260 nm) was retained and accompanied by the increase of the positive band at 290 nm and the negative band at 260 nm as the concentration of compounds increased. And it was found that differently induced CD signals appeared, respectively, with a negative band around 359 nm for **m-BQ-OHEtP**, but a positive band around 365 nm and a negative band around 430 nm for **p-BQ-OHEtP**. These results indicated that the compounds could not change the conformation of telomeric G-quadruplex DNA formed in KCl solution, but some differences for the interaction of these two compounds with G-quadruplex DNA might be existed. The same experiments were also performed for *c-kit*1 and Pu27 G-quadruplex DNA. As shown in Fig. S4, both **m-BQ-OHEtP** and **m-BQ-OHEtP** could not change the conformation of these two G-quadruplexes formed in KCl solution.

Secondly, we also tested the effect of compounds on conformation of HTG21 G-quadruplex formed in 60 mM NaCl buffer. As shown in Fig. 3A and B, in the presence of Na^+ ions and absence of the compounds, the human telomeric sequence adopted an anti-parallel conformation.[24] After addition of **m-BQ-OHEtP** to the solution, the spectrum was almost unchanged (Fig. 3A). But the addition of **p-BQ-OHEtP** resulted in a great change, with a significant decrease in the positive band at 295 nm, the disappearance of negative band and the emergence of positive band at 260 nm, and appearance of two inducing CD signals around 375 and 440 nm (Fig. 3B). The results suggested that compound **p-BQ-OHEtP** could induce anti-parallel structure of HTG21 G-quadruplex DNA to form parallel structure in the presence of Na^+ ions, but compound **m-BQ-OHEtP** didn't have this activity.

2.4.3. Effect of compounds on the conformation of G-quadruplex in the absence of salt. In order to explore whether these synthetic compounds can induce the formation of G-quadruplex structures or not in the absence of salt, the CD experiments were carried out in the absence of salt. And **m-BQ-OHEtP** and **p-BQ-OHEtP** were also selected for the following studies. On one hand, the experiment was performed for HTG21 DNA. As shown in Fig. 3C, as the concentration of **m-BQ-OHEtP** increased, the positive band at 255 nm began to decrease and the positive band at 295 increased a little. However, addition of **p-BQ-OHEtP** to the solution led to a decrease

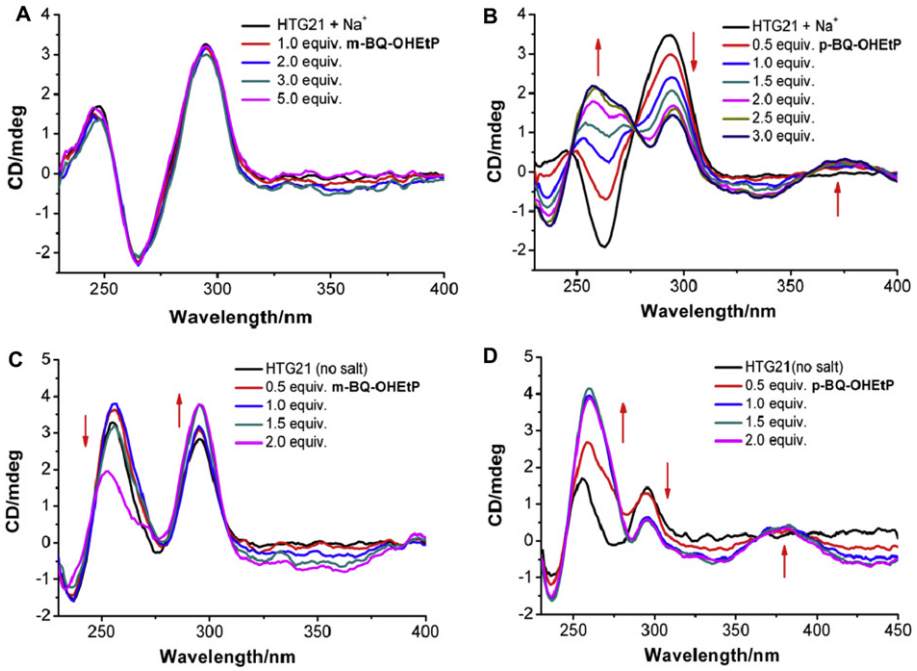

Fig. 3. CD titration spectra of ligand **m-BQ-OHEtP** (A, C) or **p-BQ-OHEtP** (B, D) in solutions of preannealed quadruplex DNA (A, B, D, 2.5 μM) and (C, 5.0 μM) in (Tris–HCl) buffer (10 mM, pH 7.4) in the presence or absence of monovalent cations. A and B, telomeric DNA (HTG21) in the presence of 60 mM NaCl. C and D, HTG21 in the absence of monovalent cation.

in the band at 295 nm, and a significant enhancement of the positive band at 260 nm (Fig. 3D). The results suggested that **m-BQ-OHEtP** had a propensity to induce formation of anti-parallel type of G-quadruplex structure and **p-BQ-OHEtP** seems more likely induced the formation of parallel type structure in the absence of salt.

On the other hand, the CD titration experiment was performed for *c-kit*1 and Pu27 DNA. As shown in Fig. S5A and S5B, *c-kit*1 sequence adopted a parallel structure in the absence of monovalent cations. Upon addition of **m-BQ-OHEtP** and **p-BQ-OHEtP**, significant changes in ellipticity were observed. And the positive band at 257 nm increased significantly with a 5 nm shift to 263 nm and the negative band at 237 nm also increased with a shift of 2 nm to 239 nm. For Pu27G-quadruplex DNA, as shown in Fig. S5C and S5D, two compounds could increase signal strength. The results indicated that both compounds could induce and stabilize the *c-kit*1 and Pu27 sequences to form parallel structure of quadruplex in the absence of salt.

2.5. Molecular modeling studies

In order to better understand how these bisquinolinium derivatives interact with telomeric G-quadruplex DNA, the molecular modeling study for the binding of compounds **m-BQ-OHEtP** and **p-BQ-OHEtP** with the HTG21 G-quadruplex DNA was carried out using AUTODOCK 4.0 program. The parallel propeller-type X-ray G-quadruplex DNA structure (PDB ID 1KF1, RCSB Protein Data Bank) was used as template for the modeling studies. For simplification, the ratio of ligand and G-quadruplex DNA was assigned to 1:1.

As shown in Fig. 4, **m-BQ-OHEtP** and **p-BQ-OHEtP** interacted with G-quadruplex DNA with a similar binding mode, the benzene ring and two methylated quinoline ring of molecule stacked onto the terminal quartet, with the nitrogen-containing side chain docked into the grooves. But there are some differences in binding mode for these two compounds, for **m-BQ-OHEtP**, the aromatic moiety of compound interacted with the G-quartet mostly across

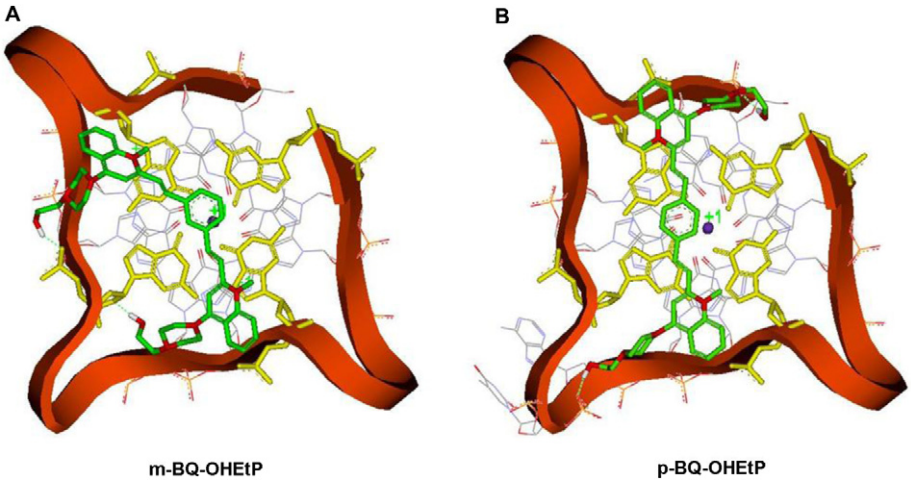

Fig. 4. Modeling studies for the complexes of the ligands (**m-BQ-OHEtP** and **p-BQ-OHEtP**) and G-quadruplex. Pictures were generated by using Discovery Studio 2.5 and were put together by Photoshop CS 2.

the diagonal line of square G-quartet by end-stacking, while for **p-BQ-OHEtP**, the aromatic moiety of the compound interacted with the G-quartet across the two lateral of the square G-quartet, which is responsible for the dimensions of the G-quadruplex and the two compounds.

The docking result showed that compound **p-BQ-OHEtP** had binding free energy of $\Delta G=-8.50$ kcal mol^{-1} and **m-BQ-OHEtP** had binding free energy of $\Delta G=-9.03$ kcal mol^{-1}. It was indicated that **m-BQ-OHEtP** had stronger stabilizing ability for telomeric G-quadruplex DNA than **p-BQ-OHEtP**, which is consistent with the results from FRET-melting curve study. As the results shown in Table S1, the calculation of ΔG of **m-BQ-OHEtP** and **p-BQ-OHEtP** for telomeric G-quadruplex DNA were −17.39 and 11.50 kJ mol^{-1}, respectively.[25]

3. Conclusion

A series of 1,3- and 1,4-disubstituted benzene bisquinolinium derivatives were designed and synthesized by a facile three-component one-pot synthesis method, which combining a Knoevenagel reaction and an S_NAr reaction to one-pot. By using this method, we can introduce two quinolinium core and two nitrogen-containing side chains to the target molecules in one step. FRET-melting results and showed their significant selectivity for G-quadruplex over duplex DNA, and their strong binding with G-quadruplex DNA.

From the CD results, we found an obvious difference of these two classes of compounds (1,3-disubstituted benzene and 1,4-disubstituted benzene derivatives) in the effect on the G-quadruplex DNA structures. Both of 1,3-disubstituted compound **m-BQ-OHEtP** and 1,4-disubstituted compound **p-BQ-OHEtP** could induce the G-quadruplex DNA to mainly form a parallel structure in co-annealed condition in presence of K^+. However, only **p-BQ-OHEtP** could convert anti-parallel G-quadruplex to its parallel form in presence of Na^+. After analyzing the possible conformational forms causing by the rotation of exocyclic single bond of two classes of compounds, we found that **m-BQ-OHEtP** had a variety of structural forms with different dimensions (from 15.4 to 19.7 Å) while **p-BQ-OHEtP** had only one dimension (20.0 Å), as shown in Fig. 5. So **m-BQ-OHEtP** has more possible combination modes to bind to the G-quadruplex than **p-BQ-OHEtP**. Derivative **p-BQ-OHEtP** with large dimension could not stabilize with anti-parallel structure for the hindrance of lateral and diagonal loops of this G-quadruplex conformation and preferentially converted such structure to parallel form. In addition, the dimensions of the compounds were also too large for the dimensions of duplex DNA. This could explain the selectivity of these two compounds to G-quadruplex over duplex DNA.

Moreover, inducing CD signal will appear when an achiral ligand binds tightly to a chiral host, such as DNA. Different induced CD signal in the spectra suggested the different binding mode of DNA binders.[20b,26] As shown in all the CD titration results, different inducing CD signals between 300 and 450 nm were observed for **m-BQ-OHEtP** and **p-BQ-OHEtP**. These inducing CD signals further suggested that both **m-BQ-OHEtP** and **p-BQ-OHEtP** interacted with HTG21 G-quadruplex DNA in a different manner. Inspired by these promising results, our research group is currently pursuing structural optimization of this class of ligands by CADD methods in parallel with organic synthesis.

4. Experimental section

4.1. Synthesis and characterization

^{1}H and ^{13}C NMR spectra were recorded using TMS as the internal standard in DMSO-d_6 or $CDCl_3$ with a Bruker BioSpin GmbH spectrometer at 400 and 100 MHz, respectively; Chemical shifts are reported in parts per million (ppm) relative to residual $CHCl_3$ (δ=7.26, ^{1}H; δ=77.0, ^{13}C) and DMSO (δ=2.50,^{1}H; δ=39.52,^{13}C) in the corresponding deuterated solvents. Mass spectra (MS) were recorded on a Shimadzu LCMS-2010A instrument with an ESI or ACPI mass selective detector, and high-resolution mass spectra (HRMS) on Shimadzu LCMS-IT-TOF. Melting points (mp) were determined using an SRS-OptiMelt automated melting point instrument without correction. Flash column chromatography was performed with silica gel (200−300 mesh) purchased from Qingdao Haiyang Chemical Co. Ltd. The purities of synthesized compounds were confirmed to be higher than 95% by analytical HPLC performed with a dual pump Shimadzu LC-20AB system equipped with an Ultimate XB-C18 column and eluted with methanol/water (70%) containing 0.1% TFA at

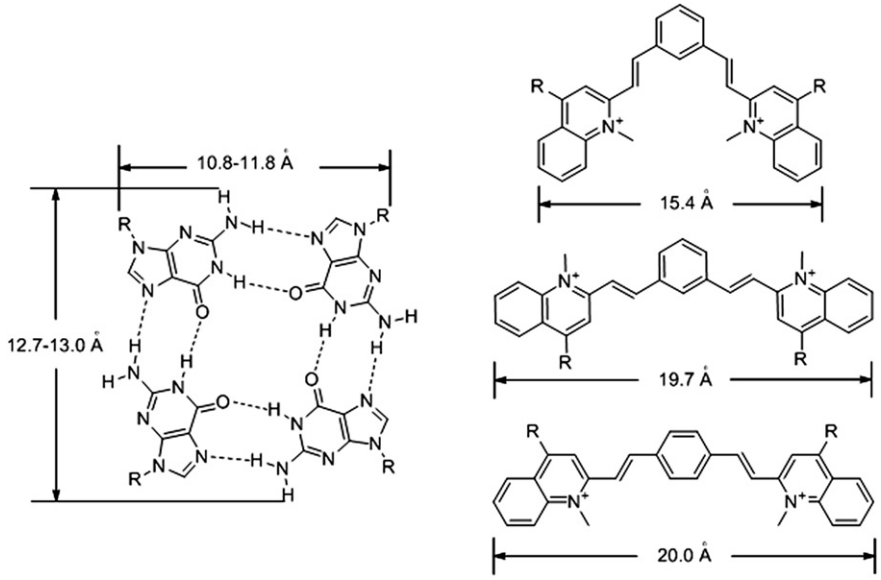

Fig. 5. Dimensions and comparison with **m-BQ-OHEtP** and **p-BQ-OHEtP**. Molecular lengths evaluated after molecular mechanics calculations (MM2, with Chem3D Ultra 8.0, CambridgeSoft Corp., MA, USA).

a flow rate of 0.3 mL min^{-1}. Aniline, ethyl acetoacetate, polyphosphoric acid, $POCl_3$ ethanol, *n*-butanol, 1,4-dioxane, THF, and all the amines were commercially available.

4.2. Synthesis of 2-methylquinolin-4-ol (1)[27]

To an equimolar solution of aniline (14.5 g, 155 mmol) and ethyl acetoacetate (20.2 g, 155 mmol) was added polyphosphoric acid (125.0 g). The reaction mixture was stirred at 130 °C for 2 h. Reaction completion was monitored by TLC. The reaction mixture was poured into ice water (500 mL) slowly with vigorous stirring. The precipitated solid was filtered and dried in vacuum oven for 4 h to get the crude product as white solid. The crude product was taken as such for the next step without further purification. Compound **1** was obtained as white solid with a yield of 77%. Mp 258.6–258.9 °C. ^{1}H NMR (400 MHz, DMSO-d_6) δ: 11.58 (s, 1H), 8.02 (d, 1H, *J*=8.0 Hz), 7.61–7.56 (m, 1H), 7.560–7.47 (m, 1H), 7.27–7.23 (m, 1H), 2.33(s, 3H). ^{13}C NMR (100 MHz, DMSO-d_6) δ: 176.67, 149.58, 140.08, 131.35, 124.73, 124.46, 122.61, 117.69, 108.33, 19.40; MS (ESI+APCI) *m*/*z*: 160.1 $[M+H]^{+1}$.

4.3. Synthesis of 4-chloro-2-methylquinoline (2)[27]

A mixture of **1** (25 g, 88.9 mmol) and freshly distilled $POCl_3$ (125 mL) was heated at 120 °C for 2 h. The reaction was monitored by TLC. After completion of the reaction, excess of $POCl_3$ was distilled off. The residue thus obtained was stirred with ice water for 15 min, then adjust the pH value to 7. And the compound was collected by filtration and washed with water. Finally purified by column chromatography with CH_2Cl_2 as eluent. Compound **2** was obtained as pale yellow solid with a yield of 65%. Mp 42.6–43.5 °C. ^{1}H NMR (400 MHz, DMSO-d_6) δ: 8.14 (d, 1H, *J*=8.0 Hz), 8.02 (d, 1H, *J*=8.0 Hz), 7.72–7.68 (m, 1H), 7.56–7.52 (m, 1H), 7.34 (s, 1H), 2.69 (s, 3H). ^{13}C NMR (100 MHz, DMSO-d_6) δ: 153.53, 143.27, 137.30, 125.10, 123.58, 121.38, 119.41, 118.60, 116.63, 19.78; MS (ESI+APCI) *m*/*z*: 179.1 $[M+H]^{+1}$.

4.4. Synthesis of 1,2-dimethyl-4-chloroquinolin-1-ium iodode (3) and 1,2-dimethyl-4-iodo-quinolin-1-ium chloride (4)[28]

A suspension of compound **2** (8.0 g, 90 mmol), iodomethane 11.2 mL (13.0 g, 180 mmol), and sulfolane (25 g) was heated in a sealed flask overnight at 80 °C. A yellow precipitate was formed. The reaction mixture was allowed to cool to room temperature and then placed in an ice bath, precipitated further with a mixture of ice cold anhydrous diethyl ether (250 mL), filtered, and washed thoroughly with anhydrous ethanol to afford **3** as a yellow solid with a yield of 90%. Compound **3**: ^{1}H NMR (400 MHz, DMSO-d_6) δ: 8.67 (d, 1H, *J*=8.0 Hz), 8.56 (d, 1H, *J*=12.0 Hz), 8.54 (s, 1H), 8.33 (t, 1H, *J*=8.0 Hz), 8.12 (t, 1H, *J*=8.0 Hz), 4.44 (s, 3H), 3.08 (s, 3H); MS (ESI+APCI) *m*/*z*: 192.1. Compound **4**: ^{1}H NMR (400 MHz, DMSO-d_6) δ: 8.90 (s, 1H), 8.56 (d, 1H, *J*=12.0 Hz), 8.26 (t, 1H, *J*=8.0 Hz), 8.05 (t, 1H, *J*=8.0 Hz), 4.36 (s, 3H), 2.99 (s, 3H); MS (ESI+APCI) *m*/*z*: 284.0.

4.5. General method for preparation of bisquinolinium derivatives

A suspension of **3** and **4** (0.64 g, 2.0 mmol), dialdehydes (terephthalaldehyde or isophthalaldehyde) (0.134 g, 1.0 mmol), and ethanol or *n*-butanol (15 mL) was heated in flask or sealed tube 3 h at 80 or 120 °C. A precipitate was formed during the process of reaction. The reaction mixture was allowed to cool to room temperature and then placed the flask or sealed tube was placed in ice bath, filtered, and washed thoroughly with anhydrous ethanol to afford bisquinolinium derivatives as a solid.

*4.5.1. Synthesis of 2,2′-((1E,1′E)-1,3-phenylenebis(ethene-2,1-diyl)) bis(1-methyl-4-(4-methylpiperazin-1-yl)-quinolin-1-ium)iodide (**m-BQ-MP**).* Following the general procedure for bisquinolinium derivatives: product was obtained as yellow-green solid. Mp 254.3–255.5 °C. ^{1}H NMR (400 MHz, DMSO-d_6) δ: 8.39 (s, 1H), 8.33 (d, 2H, *J*=8.0 Hz), 8.19 (d, 2H, *J*=8.0 Hz), 8.07 (t, 2H, *J*=8.0 Hz), 8.00 (d, 2H, *J*=4.0 Hz), 7.92 (d, 2H, *J*=16.0 Hz), 7.87 (d, 2H, *J*=16.0 Hz), 7.77 (t, 2H, *J*=8.0 Hz), 7.67 (t, 1H, *J*=8.0 Hz), 7.55 (s, 2H), 4.28 (s, 6H), 3.87 (s, 8H), 2.63 (s, 8H), 2.31(s, 6H). ^{13}C NMR (100 MHz, DMSO-d_6) δ: 159.50, 158.31, 153.47, 141.80, 140.84, 135.78, 133.92, 130.03,128.26, 126.72, 126.24, 121.17, 119.46, 119.18, 105.20, 54.27, 51.67, 45.41, 38.51. ESI-HRMS: calcd for $C_{40}H_{46}N_6^{2+}[M]^{2+}$: 305.1886; found:305.1909.

*4.5.2. Synthesis of 2,2′-((1E,1′E)-1,4-phenylenebis(ethene-2,1-diyl)) bis(1-methyl-4-(4-methylpiperazin-1-yl)-quinolin-1-ium)iodide (**p-BQ-MP**).* Following the general procedure for bisquinolinium derivatives: product was obtained as yellow-green solid. Mp 265.6–267.2 °C. ^{1}H NMR (400 MHz, DMSO-d_6) δ: 8.33 (d, 2H, *J*=8.0 Hz), 8.19 (d, 2H, *J*=8.0 Hz), 8.08 (d, 2H, *J*=4.0 Hz), 8.04 (s, 4H), 7.92 (d, 2H, *J*=16.0 Hz), 7.86 (d, 2H, *J*=16.0 Hz), 7.77 (t, 2H, *J*=8.0 Hz), 7.55 (s, 2H), 4.26 (s, 6H), 3.85 (s, 8H), 2.63 (s, 8H), 2.31 (s, 6H). ^{13}C NMR (100 MHz, DMSO-d_6) δ: 159.46, 153.46, 141.66, 140.88, 136.83, 133.88, 128.97, 126.72, 126.25, 121.35, 119.49, 119.19, 105.20, 54.25, 51.60, 45.41, 38.26. ESI-HRMS: calcd for $C_{40}H_{46}N_6^{2+}[M]^{2+}$: 305.1886; found: 305.1916.

*4.5.3. Synthesis of 2,2′-((1E,1′E)-1,3-phenylenebis(ethene-2,1-diyl)) bis(1-methylquinolin-1-ium)iodide (**m-BQ-4O**).* Following the general procedure for bisquinolinium derivatives, the product was obtained as a brown solid. Mp 264.1–265.5 °C. ^{1}H NMR (400 MHz, DMSO-d_6) δ: 9.18 (d, 2H, *J*=8.0 Hz), 8.64 (d, 4H, *J*=8.0 Hz), 8.53 (s, 1H), 8.42 (d, 2H, *J*=8.0 Hz), 8.28–8.23 (m, 4H), 8.16 (d, 2H, *J*=8.0 Hz), 8.10 (d, 2H, *J*=16.0 Hz), 8.02 (t, 2H, *J*=6.0 Hz), 7.76 (t, 1H, *J*=8.0 Hz), 4.65 (s, 6H). ^{13}C NMR (100 MHz, DMSO-d_6) δ: 155.90, 145.53, 144.60, 139.21, 135.62, 135.13, 131.41, 130.11, 129.87, 129.34, 129.27, 128.03, 121.37, 120.68, 119.44, 40.46. ESI-HRMS: calcd for $C_{30}H_{26}N_2^{2+}[M]^{2+}$: 207.1043; found:207.1052.

*4.5.4. Synthesis of 2,2′-((1E,1′E)-1,3-phenylenebis(ethene-2,1-diyl)) bis(4-(4-(2-hydroxyethyl)piperazin-1-yl)-1-methylquinolin-1-ium) iodide (**m-BQ-OHEtP**).* Following the general procedure for bisquinolinium derivatives, the product was obtained as a yellow-green solid. Mp 215.8–216.7 °C. ^{1}H NMR (400 MHz, DMSO-d_6) δ: 8.56 (s, 1H), 8.38 (d, 2H, *J*=12.0 Hz), 8.23 (d, 2H, *J*=8.0 Hz), 8.10 (t, 2H, *J*=8.0 Hz), 8.03 (m, 4H), 7.95 (d, 2H, *J*=16.0 Hz), 7.80 (t, 2H, *J*=8.0 Hz), 7.68 (t, 1H, *J*=8.0 Hz), 7.63 (s, 2H), 4.34 (s, 6H), 3.97 (s, 8H), 3.72 (s, 4H), 2.34 (s, 12H). ^{13}C NMR (100 MHz, DMSO-d_6) δ: 159.27, 153.82, 142.28, 140.72, 135.75, 134.06, 130.33, 129.53, 128.21, 126.65, 126.56, 121.06, 119.60, 119.31, 105.78, 58.74, 56.85, 56.64, 51.79, 50.08, 38.83. ESI-HRMS: calcd for $C_{42}H_{50}N_6O_2^{2+}[M]^{2+}$: 335.1992; found:335.2009.

*4.5.5. Synthesis of 2,2′-((1E,1′E)-1,4-phenylenebis(ethene-2,1-diyl)) bis(1-methylquinolin-1-ium)iodide (**p-BQ-4O**).* Following the general procedure for bisquinolinium derivatives, the product was obtained as a brown solid. Mp 296.5–297.8 °C. ^{1}H NMR (400 MHz, DMSO-d_6) δ: 9.15 (d, 2H, *J*=8.0 Hz), 8.62 (d, 4H, *J*=8.0 Hz), 8.40 (d, 2H, *J*=8.0 Hz), 8.24 (t, 4H, *J*=12.0 Hz), 8.17 (s, 4H), 8.11 (d, 2H, *J*=16.0 Hz), 8.00 (t, 2H, *J*=8.0 Hz), 4.62 (s, 6H). $C_{30}H_{26}N_2^{2+}[M]^{2+}$: 207.1043; found:207.1041.

*4.5.6. Synthesis of 2,2′-((1E,1′E)-1,4-phenylenebis(ethene-2,1-diyl)) bis(1-methyl-4-morpholinoquinolin-1-ium) iodide (**p-BQ-Mor**).* Following the general procedure for bisquinolinium derivatives, the product was obtained as a brown solid. Mp 296.5–297.7 °C. ^{1}H NMR (400 Hz, DMSO-d_6) δ: 8.35 (d, 2H, *J*=12.0 Hz), 8.23 (d, 2H, *J*=8.0 Hz),

8.08 (t, 2H, *J*=6.0 Hz), 8.04 (s, 4H), 7.93(d, 2H, *J*=16.0 Hz), 7.87(d, 2H, *J*=16.0 Hz), 7.77 (t, 2H, *J*=8.0 Hz), 7.56 (s, 2H), 4.28 (s, 6H), 3.90 (d, 8H, *J*=4.0 Hz), 3.87 (d, 8H, *J*=4.0 Hz). ESI-HRMS: calcd for $C_{38}H_{40}N_4O_2^{2+}[M]^{2+}$: 292.1570; found: 292.1589.

*4.5.7. Synthesis of 2,2′-((1E,1′E)-1,4-phenylenebis(ethene-2,1-diyl)) bis(4-(4-(2-hydroxyethyl)piperazin-1-yl)-1-methylquinolin-1-ium) iodide (**p-BQ-OHEtP**).* Following the general procedure for bisquinolinium derivatives, the product was obtained as a yellow-green solid. Mp 236.9–238.2 °C. ^{1}H NMR (400 MHz, DMSO-d_6) δ: 8.32 (d, 2H, *J*=8.0 Hz), 8.19 (d, 2H, *J*=8.0 Hz), 8.07 (d, 2H, *J*=8.0 Hz), 8.04 (s, 4H), 7.86 (d, 2H, *J*=16.0 Hz), 7.76 (t, 2H, *J*=8.0 Hz), 7.53 (s, 2H), 4.53 (t, 2H), 4.26 (s, 6H), 3.86 (s, 8H), 3.61–3.57 (m, 4H), 2.75 (s, 8H), 2.54 (t, 4H, *J*=4.0 Hz). ^{13}C NMR (100 MHz, DMSO-d_6) δ: 159.32, 153.40, 141.61, 140.86, 136.81, 133.89, 128.97, 126.73, 126.18, 121.33, 119.40, 119.17, 105.08, 98.25, 59.79, 58.54, 52.83, 51.77. ESI-HRMS: calcd for $C_{46}H_{60}N_8^{2+}[M]^{2+}$: 335.1992; found:335.1988.

*4.5.8. Synthesis of 2,2′-((1E,1′E)-1,3-phenylenebis(ethene-2,1-diyl)) bis(1-methyl-4-morpholinoquinolin-1-ium) iodide (**m-BQ-Mor**).* Following the general procedure for bisquinolinium derivatives, the product was obtained as a brown solid. Mp 309.8–311.5 °C. ^{1}H NMR (400 MHz, DMSO-d_6) δ: 8.41 (s, 1H), 8.35 (d, 2H, *J*=8.0 Hz), 8.24 (d, 2H, *J*=8.0 Hz), 8.08 (t, 2H, *J*=4.0 Hz), 8.01 (d, 2H, *J*=8.0 Hz), 7.95 (d, 2H, *J*=16.0 Hz), 7.89 (d, 2H, *J*=16.0 Hz), 7.78 (t, 2H, *J*=8.0 Hz), 7.68 (t, 1H, *J*=8.0 Hz), 7.57 (s, 2H), 4.30 (s, 6H), 3.90 (s, 8H), 3.88 (s, 8H). ^{13}C NMR (100 MHz, DMSO-d_6) δ: 159.56, 153.68, 143.58, 142.00, 140.83, 135.80, 133.98, 130.06, 126.71, 126.38, 121.15, 119.43, 119.26, 113.22, 105.26, 65.82, 52.11, 34.63. ESI-HRMS: calcd for $C_{38}H_{40}N_4O_2^{2+}[M]^{2+}$: 292.1570; found:292.1565.

*4.5.9. Synthesis of 2,2′-((1E,1′E)-1,3-phenylenebis(ethene-2,1-diyl)) bis(1-methyl-4-(pyrrolidin-1-yl)quinolin-1-ium)iodide (**m-BQ-Pyrro**).* Following the general procedure for bisquinolinium derivatives, the product was obtained as a brown solid. Mp 314.1–316.2 °C. ^{1}H NMR (400 MHz, DMSO-d_6) δ: 8.56 (d, 2H *J*=8.0 Hz), 8.32 (d, 1H, *J*=8.0 Hz), 8.20 (d, 2H, *J*=8.0 Hz), 8.03 (t, 2H, *J*=8.0 Hz), 7.94 (d, 2H, *J*=8.0 Hz), 7.80 (d, 4H, *J*=4.0 Hz), 7.70 (t, 2H, *J*=8.0 Hz), 7.64 (t, 1H, *J*=8.0 Hz), 7.05 (s, 2H), 4.15 (s, 6H), 4.05 (s, 8H), 2.08 (s, 8H). ^{13}C NMR (100 MHz, DMSO-d_6) δ: 154.48, 151.78, 140.70, 140.24, 135.87, 133.44, 129.54, 127.80, 127.25, 124.99, 121.62, 118.17, 112.01, 111.96, 100.69, 53.58, 37.97, 25.12. ESI-HRMS: calcd for $C_{38}H_{40}N_4^{2+}[M]^{2+}$: 276.1621; found: 276.1634.

*4.5.10. Synthesis of 2,2′-((1E,1′E)-1,4-phenylenebis(ethene-2,1-diyl)) bis(1-methyl-4-(pyrrolidin-1-yl)quinolin-1-ium)iodide (**p-BQ-Pyrro**).* Following the general procedure for bisquinolinium derivatives, the product was obtained as a brown solid. Mp 307.2–308.5 °C. ^{1}H NMR (400 MHz, DMSO-d_6) δ: 8.56 (d, 2H, *J*=12.0 Hz), 8.20 (d, 2H, *J*=8.0 Hz), 8.03 (t, 2H, *J*=8.0 Hz), 7.98 (s, 4H), 7.79 (s, 4H, *J*=8.0 Hz), 7.70 (t, 2H, *J*=4.0 Hz), 7.05 (s, 2H), 4.13 (s, 6H), 4.05 (s, 8H), 2.08 (s, 8H). ^{13}C NMR (100 MHz, DMSO-d_6) δ: 154.44, 151.78, 145.35, 140.73, 140.06, 136.66, 133.43, 128.71, 127.23, 124.97, 121.69, 118.17, 100.66, 53.46, 37.84, 25.09. ESI-HRMS: calcd for $C_{38}H_{40}N_4^{2+}[M]^{2+}$: 276.1621; found: 276.1638.

*4.5.11. Synthesis of 2,2′-((1E,1′E)-1,4-phenylenebis(ethene-2,1-diyl)) bis(4-((2-(dimethylamino)ethyl)amino)-1-methylquinolin-1-ium)iodide (**p-BQ-DM-EA**).* Following the general procedure for bisquinolinium derivatives, the product was obtained as a yellow-green solid. Mp 307.4–308.2 °C. ^{1}H NMR (400 MHz, DMSO-d_6) δ: 9.88 (s, 2H), 9.12 (s, 2H), 8.67 (d, 2H, *J*=8.0 Hz), 8.30 (d, 2H, *J*=8.0 Hz), 8.07 (s, 4H), 7.94 (d, 2H, *J*=16.0 Hz), 7.87 (d, 2H, *J*=16.0 Hz), 7.30 (s, 2H), 4.23 (s, 6H), 4.10 (s, 4H), 3.51 (s, 4H), 2.93 (s, 12H). ^{13}C NMR (100 MHz, DMSO-d_6) δ: 154.38, 154.06, 141.36, 139.35, 136.74, 134.17, 128.90, 126.49, 123.71, 121.67, 119.03, 117.53, 98.04, 54.41, 42.78, 38.17, 37.94. ESI-HRMS: calcd for $C_{38}H_{46}N_6^{2+}[M]^{2+}$: 293.1886; found: 293.1899.

*4.5.12. Synthesis of 2,2′-((1E,1′E)-1,3-phenylenebis(ethene-2,1-diyl)) bis(4-((2-(dimethylamino)ethyl)amino)-1-methylquinolin-1-ium)iodide (**m-BQ-DM-EA**).* Following the general procedure for bisquinolinium derivatives, the product was obtained as a yellow-green solid. Mp 271.2–272.4 °C. ^{1}H NMR (400 MHz, DMSO-d_6) δ: 9.13 (s, 1H), 8.59 (d, 2H, *J*=8.0 Hz), 8.30 (d, 2H, *J*=8.0 Hz), 8.10 (t, 2H, *J*=8.0 Hz), 7.86 (d, 2H, *J*=16.0 Hz), 7.85 (t, 2H, *J*=8.0 Hz), 7.67 (t, 1H, *J*=8.0 Hz), 4.25 (s, 6H), 4.10 (s, 2H), 3.50 (s, 8H), 2.92 (s, 12H). ^{13}C NMR (100 MHz, DMSO-d_6) δ: 154.09, 141.58, 139.34, 135.83, 134.14, 130.07, 129.49, 127.87, 126.47, 123.87, 121.46, 119.01, 117.53, 99.49, 97.98, 54.40, 42.73, 38.27, 38.18. ESI-HRMS: calcd for $C_{38}H_{46}N_6^{2+}[M]^{2+}$: 293.1886; found: 293.1898.

*4.5.13. Synthesis of 2,2′-((1E,1′E)-1,4-phenylenebis(ethene-2,1-diyl)) bis(4-((2-(diethylamino)ethyl)amino)-1-methylquinolin-1-ium)iodide (**p-BQ-DE-EA**).* Following the general procedure for bisquinolinium derivatives, the product was obtained as a yellow-green solid. Mp 307.4.3–308.5 °C. ^{1}H NMR (400 MHz, DMSO-d_6) δ: 9.52 (s, 2H), 9.04 (s, 2H), 8.54 (d, 2H, *J*=8.0 Hz), 8.30 (d, 2H, *J*=8.0 Hz), 8.06 (s, 4H), 7.93 (d, 2H, *J*=16.0 Hz), 7.85 (d, 2H, *J*=16.0 Hz), 7.28 (s, 2H), 4.23 (s, 6H), 4.09 (t, 4H, *J*=12.0 Hz), 3.52 (s, 12H), 1.24 (s, 12H). ^{13}C NMR (100 MHz, DMSO-d_6) δ: 154.02, 141.31, 139.40, 136.73, 134.18, 128.91, 126.61, 123.53, 121.70, 120.19, 119.11, 117.46, 97.97, 48.59, 46.58, 38.35, 37.96, 8.45. ESI-HRMS: calcd for $C_{42}H_{54}N_6^{2+}[M]^{2+}$: 321.2199; found: 321.2204.

*4.5.14. Synthesis of 2,2′-((1E,1′E)-1,3-phenylenebis(ethene-2,1-diyl)) bis(4-((2-(diethylamino)ethyl)amino)-1-methylquinolin-1-ium)iodide (**m-BQ-DE-EA**).* Following the general procedure for bisquinolinium derivatives, the product was obtained as a yellow-green solid. Mp 289.7–291.3 °C. ^{1}H NMR (400 Hz, DMSO-d_6) δ: 9.07 (s, 1H), 8.58 (d, 2H, *J*=8.0 Hz), 8.31 (d, 2H, *J*=8.0 Hz), 8.09 (t, 2H, *J*=8.0 Hz), 8.01 (t, 2H, *J*=8.0 Hz), 7.94 (d, 2H, *J*=16.0 Hz), 7.84 (t, 2H, *J*=8.0 Hz), 7.65 (t, 1H, *J*=8.0 Hz), 7.31 (s, 2H), 4.27 (s, 6H), 4.16 (s, 2H), 3.35 (s, 16H), 1.27 (s, 12H). ^{13}C NMR (100 MHz, DMSO-d_6) δ: 154.44, 153.98, 141.54, 139.34, 135.77, 134.17, 130.14, 129.44, 127.92, 126.59, 123.61, 121.42, 119.10, 117.46, 97.96, 48.80, 46.64, 38.35, 38.09, 8.67. ESI-HRMS: calcd for $C_{42}H_{54}N_6^{2+}[M]^{2+}$: 321.2199; found: 321.2208.

4.6. FRET-melting experiments

To evaluate the stabilization and selectivity of bisquinolinium derivatives for G-quadruplex DNA, FRET-melting experiments were carried out. The human telomeric G-quadruplex DNA [F21T, 5′-FAM-d(GGG[TTAGGG]$_3$)-TAMRA-3′] and two oncogene promoter G-quadruplexes c-myc [F22T, FAM-d(5′-TGAG$_3$TG$_3$TAG$_3$TG$_3$TA$_2$)-TAMRA-3′], c-kit1[F-c-kit1-T, 5′-FAM-d(AGGGAGGGCGCTGGG-AGGAGGG)-TAMRA-3′] containing fluorophores at both 5′-end and 3′-end were used in this assay. A sequence that forms hairpin duplex DNA structure F10T (5′-FAM-dTATAGCTATAHEGTATAGC-TATATAMRA-3′) as a non-quadruplex control was also involved. The melting temperature of all G-quadruplexes was determined in the presence of 1 μM of bisqinolinium derivatives in Tris–HCl buffer containing 60 mM KCl. The result of FRET-melting assay was represented as enhanced melting temperature (ΔT_m) reported in Table 1. The melting of the G-quadruplex was monitored alone or in the presence of various compounds. Final analysis of the data was carried out using Excel and Origin 7.5 (OriginLab Corp.).

4.7. TO FIDs assay

Thiazole orange (TO) was purchased from Aldrich and used without further purification. Three quadruplex-forming

oligonucleotides used were: HTG21, Pu27. And duplex DNA ds26 was also used. The oligonucleotides were annealed at 10 mm in K^+ buffer, containing lithium cacodylate (10 mm) at pH 7.3 and KCl (100 mm), by heating at 95 °C for 5 min and cooling over ice to favor the intramolecular folding by kinetic trapping. The duplex DNA ds26 was prepared by heating the self-complementary strand at 95 °C followed by a slow cooling to room temperature over 3 h. Each experiment was performed in a cell with a path length of 1 cm in K^+ buffer with a total volume of 1.25 mL. The FID assay was designed as follows: 0.25 mm prefolded DNA is mixed with TO (0.250 μM for HTG21 and Pu27; 0.50 μM for ds26). Each ligand-addition step (11 steps of 4.0 mL, from 0.2 to 10 equiv) was followed by a 3 min equilibration period after which the fluorescence spectrum was recorded with the background subtracted. The percentage of displacement was calculated from the fluorescence area (FA, 510–750 nm, Ex=501 nm) by using percentage of displacement=$100-[(FA/FA_0)\times 100]$, with FA_0 being the fluorescence of TO bound to DNA without added ligand. The percentage of displacement was plotted as a function of the concentration of added ligand. Final analysis of the data was carried out by using Excel and Origin 7.5 software.

4.8. CD measurements experiments

CD measurements were performed on a Chirascan circular dichroism spectrophotometer (Applied Photophysics) using a quartz cuvettes of 2 mm optical path length and over a wavelength range of 230–450 nm at 1 nm bandwidth, 1 nm step size, and 0.5 s time per point. The oligomer HTG21 (GGGTTAGGGTTAGGGTTAGGG) at a final concentration of 5 μM was resuspended in Tris–HCl buffer (10 mM, pH 7.4) containing the specific cations and the compounds to be tested. The samples were heated to 95 °C for 5 min, then gradually cooled to room temperature and incubated at 4 °C overnight. A buffer baseline was collected in the same cuvette and subtracted from the sample spectra. The CD spectra were obtained by taking the average of at least three scans at 25 °C. Then, CD titration was performed at a fixed HTG21 concentration (2.5 μM) with various concentrations of the compounds in Tris–HCl buffer in the absence or in the presence of 60 mM KCl or NaCl. After each addition of compound, the reaction mixture was stirred and allowed to equilibrate for at least 5 min (until no elliptic changes were observed) and a CD spectrum was collected. Final analysis of the data was carried out using Origin 7.5 (OriginLab Corp.).

The CD experiments for DNA oligomers HTG21, Pu27 (TGGGGAGGGTGGGGAGGGTGGGGAAGG), and *c-kit1* (AGGGAGGGCGCTGGGAGGAGGG) were also carried out at a final concentration of 5 μM in 10 mM Tris–HCl buffer, pH 7.4 at 25 °C containing the tested ligands (25 μM) in the absence or presence of KCl or NaCl. In the presence of 150 mM KCl, The samples containing HTG21(5 μM) and compounds (25 μM) in 10 mM Tris–HCl buffer, pH 7.4, were annealed by heating at 95 °C for 5 min, and then gradually cooled to room temperature and incubated at 4 °C overnight. The recording of CD spectra was carried out following the CD experiment. For CD titration experiments, the samples containing HTG21, Pu27 and c-kit1 DNA (2.5 μM) in 10 mM Tris–HCl buffer in the absence of salt or the presence of 60 mM KCl or NaCl, pH 7.4, were annealed by heating at 95 °C for 5 min, and then gradually cooled to room temperature and incubated at 4 °C overnight. The recording of CD spectra was carried out following the CD experiment.

4.9. Molecular modeling study

Docking studies were carried out using the AUTODOCK 4.0 program.[29] By using ADT,[30] nonpolar hydrogens of telomeric G-quadruplex were merged to their corresponding carbons, and partial atomic charges were assigned. The nonpolar hydrogens of the ligands were merged, and rotatable bonds were assigned. The resulting G-quadruplex structure was used as an input for the AUTOGRID program. AUTOGRID gave a precalculated atomic affinity grid map for each atom type in the ligand, plus an electrostatics map, and a separate desolvation map present in the substrate molecule. The dimensions of the active site box, which was placed at the center of the G-quadruplex, were set to 60 Å×60 Å×60 Å with the grid points 0.375 Å apart. Docking calculations were carried out using the Lamarckian genetic algorithm (LGA). Initially, we used a population of random individuals (population size: 150), a maximum number of 25,000,000 energy evaluations, a maximum number of generations of 27,000, and a mutation rate of 0.02. One hundred independent docking runs were carried out for each ligand. The resulting positions were clustered according to a root-mean-square criterion of 0.5 Å.

Acknowledgements

We thank the Natural Science Foundation of China (21172272, 91213302), the Specialized Research Fund for the Doctoral Program of Higher Education (20110171110051), and the Science Foundation of Guangzhou (2009A1-E011-6) for financial support of this study.

Supplementary data

Supplementary data associated with this article can be found in the online version, at http://dx.doi.org/10.1016/j.tet.2013.04.045.

References and notes

1. (a) Lipps, H. J.; Rhodes, D. *Trends Cell Biol.* **2009**, *19*, 414–422; (b) Huppert, J. L. *Chem. Soc. Rev.* **2008**, *37*, 1375–1384.
2. (a) Cogoi, S.; Xodo, L. E. *Nucleic Acids Res.* **2006**, *34*, 2536–2549; (b) Todd, A. K.; Johnston, M.; Neidle, S. *Nucleic Acids Res.* **2005**, *33*, 2901–2907; (c) Qin, Y.; Rezler, E. M.; Gokhale, V.; Sun, D.; Hurley, L. H. *Nucleic Acids Res.* **2007**, *35*, 7698–7713; (d) Bejugam, M.; Sewitz, S.; Shirude, P. S.; Rodriguez, R.; Shahid, R.; Balasubramanian, S. *J. Am. Chem. Soc.* **2007**, *129*, 12926–12927; (e) Huppert, J. L.; Balasubramanian, S. *Nucleic Acids Res.* **2005**, *33*, 2908–2916; (f) Huppert, J. L.; Balasubramanian, S. *Nucleic Acids Res.* **2006**, *35*, 406–413.
3. (a) Siddiqui-Jain, A.; Grand, C. L.; Bearss, D. J.; Hurley, L. H. *Proc. Natl. Acad. Sci. U. S.A.* **2002**, *99*, 11593–11598; (b) Phan, A. T.; Kuryavyi, V.; Gaw, H. Y.; Patel, D. J. *Nat. Chem. Biol.* **2005**, *1*, 167–173; (c) Yang, D.; Hurley, L. H. *Nucleosides Nucleotides Nucleic Acids* **2006**, *25*, 951–968; (d) Phan, A. T.; Modi, Y. S.; Patel, D. J. *J. Am. Chem. Soc.* **2004**, *126*, 8710–8716; (e) Kumar, N.; Basundra, R.; Maiti, S. *Nucleic Acids Res.* **2009**, *37*, 103321–103331; (f) Thakur, R. K.; Kumar, P.; Halder, K.; Verma, A.; Kar, A.; Parent, J. L.; Basundra, R.; Kumar, A.; Chowdhury, S. *Nucleic Acids Res.* **2009**, *37*, 172–183; (g) Simonsson, T.; Pecinka, P.; Kubista, M. *Nucleic Acids Res.* **1998**, *26*, 1167–1172.
4. (a) Rankin, S.; Reszka, A. P.; Huppert, J.; Zloh, M.; Parkinson, G. N.; Todd, A. K.; Ladame, S.; Balasubramanian, S.; Neidle, S. *J. Am. Chem. Soc.* **2005**, *127*, 10584–10589; (b) Fernando, H.; Reszka, A. P.; Huppert, J.; Ladame, S.; Rankin, S.; Venkitaraman, A. R.; Neidle, S.; Balasubramanian, S. *Biochemistry* **2006**, *45*, 7854–7860; (c) Waller, Z. A. E.; Sewitz, S. A.; Hsu, S. T.; Balasubramanian, S. *J. Am. Chem. Soc.* **2009**, *131*, 12628–12633.
5. (a) Ou, T.-M.; Lu, Y.-J.; Huang, Z.-S.; Wang, X.-D.; Tan, J.-H.; Chen, Y.; Ma, D.-L.; Wong, K.-Y.; Tang, J.-C.; Chan, A.-S.; Gu, L.-Q. *J. Med. Chem.* **2007**, *50*, 1465–1474; (b) Cogoi, S.; Paramasivam, M.; Spolaore, B.; Xodo, L. E. *Nucleic Acids Res.* **2008**, *36*, 3765–3780.
6. (a) Collie, G. W.; Parkinson, G. N. *Chem. Soc. Rev.* **2011**, *40*, 5867–5892; (b) Xu, Y. *Chem. Soc. Rev.* **2011**, *40*, 2719–2740.
7. Balasubramanian, S.; Hurley, L. H.; Neidle, S. *Nat. Rev. Drug Discov.* **2011**, *10*, 261–275.
8. Zahler, A. M.; Williamson, J. R.; Cech, T. R.; Prescott, D. M. *Nature* **1991**, *350*, 718–720.
9. Neidle, S. *Curr. Opin. Struct. Biol.* **2009**, *19*, 239–250.
10. (a) Granotier, C.; Pennarun, G.; Riou, L.; Hoffschir, F.; Gauthier, L. R.; De Cian, A.; Gomez, D.; Mandine, E.; Riou, J.-F.; Mergny, J.-L.; Mailliet, P.; Dutrillaux, B.; Boussin, F. D. *Nucleic Acids Res.* **2005**, *33*, 4182–4190; (b) Rodriguez, R.; Mller, S.; Yeoman, J. A.; Trentesaux, C.; Riou, J.-F.; Balasubramanian, S. *J. Am. Chem. Soc.* **2008**, *130*, 15758–15759.
11. Czerwinska, I.; Juskowiak, B. *Int. J. Biol. Macromol.* **2012**, *51*, 576–582.
12. Peng, D.; Tan, J.-H.; Chen, S.-B.; Ou, T.-M.; Gu, L.-Q.; Huang, Z.-S. *Bioorg. Med. Chem.* **2010**, *18*, 8235–8242.
13. Müller, S.; Sanders, D. A.; Di Antonio, M.; Matsis, S.; Riou, J.-F.; Rodriguez, R.; Balasubramaniana, S. *Org. Biomol. Chem.* **2012**, *10*, 6537–6546.

14. Mullins, S. T.; Annan, N. K.; Cook, P. R.; Lowe, G. *Biochemistry* **1992**, *31*, 842–849.
15. Yamashita, K.; Tanaka, T.; Hayashi, M. *Tetrahedron* **2005**, *61*, 7981–7985.
16. (a) Mergny, J.-L.; Lacroix, L.; Teulade-Fichou, M.-P.; Hounsou, C.; Guittat, L.; Hoarau, M.; Arimondo, P. B.; Vigneron, J.-P.; Lehn, J.-M.; Riou, J.-F.; Garestier, T.; Helene, C. *Proc. Natl. Acad. Sci. U.S.A.* **2001**, *98*, 3062–3067; (b) De Cian, A.; Guittat, L.; Kaiser, M.; Sacca, B.; Amrane, S.; Bourdoncle, A.; Alberti, P.; Teulade-Fichou, M. P.; Lacroix, L.; Mergny, J. L. *Methods* **2007**, *42*, 183–195.
17. (a) Shirude, P. S.; Gillies, E. R.; Ladame, S.; Godde, F.; Shin-ya, K.; Huc, I.; Balasubramanian, S. *J. Am. Chem. Soc.* **2007**, *129*, 11890–11891; (b) Mueller, S.; Pantos, G. D.; Rodriguez, R.; Balasubramanian, S. *Chem. Commun.* **2009**, 80–82.
18. Monchaud, D.; Allain, C.; Bertrand, H.; Smargiasso, N.; Rosu, F.; Gabelica, V.; De Cian, A.; Mergny, J. L.; Teulade-Fichou, M. P. *Biochimie* **2008**, *90*, 1207–1223.
19. Monchaud, D.; Allain, C.; Teulade-Fichou, M. P. *Bioorg. Med. Chem. Lett.* **2006**, *16*, 4842–4845.
20. (a) Paramasivan, S.; RuJan, I.; Bolton, P. H. *Methods* **2007**, *43*, 324–331; (b) White, E. W.; Tanious, F.; Ismail, M. A.; Reszka, A. P.; Neidle, S.; Boykin, D. W.; Wilson, W. D. *Biophys. Chem.* **2007**, *126*, 140–153.
21. (a) Tan, J.-H.; Ou, T.-M.; Hou, J.-Q.; Lu, Y.-J.; Huang, S.-L.; Luo, H.-B.; Wu, J.-Y.; Huang, Z.-S.; Wong, K.-Y.; Gu, L.-Q. *J. Med. Chem.* **2009**, *52*, 2825–2835; (b) Moorhouse, A. D.; Santos, A. M.; Gunaratnam, M.; Moore, M.; Neidle, S.; Moses, J. E. *J. Am. Chem. Soc.* **2006**, *128*, 15972–15973.
22. (a) Dash, J.; Waller, Z. A. E.; Pantos, G. D.; Balasubramanian, S. *Chem.—Eur. J.* **2011**, *17*, 4571–4581; (b) Kaluzhny, D.; Ilyinsky, N.; Shchekotikhin, A.; Sinkevich, Y.; Tsvetkov, P. O.; Tsvetkov, V.; Veselovsky, A.; Livshits, M.; Borisova, O.; Shtil, A.; Shchyolkina, A. *PloS One* **2011**, *6* e271511–6.
23. Ou, T.-M.; Lu, Y.-J.; Tan, J.-H.; Huang, Z.-S.; Wong, K.-Y.; Gu, L.-Q. *ChemMedChem* **2008**, *3*, 690–713.
24. (a) Wang, Y.; Patel, D. J. *Structure* **1993**, *1*, 263–282; (b) Rezler, E. M.; Seenisamy, J.; Bashyam, S.; Kim, M. Y.; White, E.; Wilson, W. D.; Hurley, L. H. *J. Am. Chem. Soc.* **2005**, *127*, 9439–9447.
25. (a) Rachwal, P. A.; Fox, K. R. *Methods* **2007**, *43*, 291–301; (b) Lane, A. N.; Chaires, J. B.; Gray, R. D.; Trent, J. O. *Nucleic Acids Res.* **2008**, *36*, 5482–5515.
26. Dash, J.; Shirude, P. S.; Hsu, S.-T. D.; Balasubramanian, S. *J. Am. Chem. Soc.* **2008**, *130*, 15950–15956.
27. (a) Eswaran, S.; Adhikari, A. V.; Chowdhury, I. H.; Pal, N. K.; Thomasa, K. D. *Eur. J. Med. Chem.* **2010**, *45*, 3374–3383; (b) Ong, C. W.; Liu, M.-C.; Lee, K.-D.; Chang, K. W.; Yang, Y.-T.; Tung, H.-W.; Fox, K. R. *Tetrahedron* **2012**, *68*, 5453–5457.
28. Lu, Y.-J.; Ou, T.-M.; Tan, J. H.; Hou, J.-Q.; Shao, W.-Y.; Peng, D.; Sun, N.; Wang, X.-D.; Wu, W.-B.; Bu, X.-Z.; Huang, Z.-S.; Ma, D.-L.; Wong, K.-Y.; Gu, L.-Q. *J. Med. Chem.* **2008**, *51*, 6381–6392.
29. Morris, G. M.; Goodsell, D. S.; Halliday, R. S.; Huey, R.; Hart, W. E.; Belew, R. K.; Olson, A. J. *J. Comput. Chem.* **1998**, *19*, 1639–1662.
30. Sanner, M. F. *J. Mol. Graph. Model.* **1999**, *17*, 57–61.